A Corrosion Study of Grain-Refined 304L Stainless Steels Produced by the Martensitic Process

M. Atapour [1*], M.M. Dana [2], F. Ashrafizadeh [3]

Department of Materials Engineering, Isfahan University of Technology, Isfahan 84156-83111, Iran

Abstract

AISI 304L austenitic stainless steel with different grain sizes of 0.5-12 μm was obtained through the martensitic process. Corrosion behavior of different samples was investigated in a 0.5M HCl solution using open circuit potential, potentiodynamic polarization and electrochemical impedance spectroscopy tests. Also, the correlation between the grain size and pitting corrosion resistance was assessed by cyclic polarization experiments and immersion tests combined with optical microscopy. The potentiodynamic polarization results demonstrated that grain refinement had little influence on the corrosion potential and corrosion current density. However, cyclic polarization tests showed that the ultrafine grained steel (500 nm grain size) exhibited superior pitting resistance, as compared to the steel with the larger grain size (1-12 μm). This behavior was confirmed by immersion tests in the 0.5M HCl for 48 hours, thereby showing that the size and the number of pits were decreased by increasing the grain size. The electrochemical impedance spectroscopy results also revealed that grain refinement enhanced the stability of the passive film of 304L stainless steel.

Keywords: Ultra-fine grained stainless steel; Corrosion, Pitting corrosion resistance; Grain size.

1. Introduction

Austenitic stainless steels are well known structural materials due to their unique combination of such properties as reasonable corrosion resistance, suitable ductility and good weldability. Owing to these advantages, austenite stainless steels have been widely used in many industrial applications like oil and petrochemical fields, chemical plants, biomedical implants and food industries [1]. The corrosion resistance of these materials arises from a passive film on the surface which is essentially composed of oxides and hydroxides of iron and chromium [2, 3]. However, the low pitting resistance of these steels, particularly in the presence of chloride ions, limits many of their applications. In this respect, many attempts have been made to improve the localized corrosion resistance of austenitic stainless steels. A plethora of studies have been focused on coatings [4-6] and surface modification techniques [7-9].

Recently, bulk nano and ultrafine grained (UFG) materials have gained much popularity and acceptance since they provide the benefit of greatly increasing both strength and fracture toughness. However, due to high recrystallization temperature (above 900 ˚C), the use of common grain refinement processes has been limited to austenitic stainless steels [10].

Martensitic transformation has been proposed as an effective thermomechanical process that can be successfully applied to austenitic stainless steels for manufacturing ultrafine grain microstructures [11, 12].

As it is well established, the inherent changes associated with grain refinement, such as grain boundary density, orientation and residual stress, can significantly influence the electrochemical behavior of materials [13]. Accordingly, a large number of investigations have addressed the effect of grain size on corrosion. Most of the studies reporting a number of light metals (Mg, Al, and Ti) and transition metals (Fe/steel, Co, Ni, Cu, and Zn) can be found in an excellent review conducted by Ralston and Birbilis [13]. They have concluded that it is difficult to establish a general relationship between grain size and corrosion resistance.

Although the mechanical properties of nano and UFG austenitic stainless steels have been studied extensively, relatively few investigations have been conducted to examine the influence of the grain size on the corrosion resistance of this class of materials [14, 15]. Di Schino and Kenny [16] studied the effect of grain size on the uniform and pitting corrosion behavior of 304 stainless steel in a 3.5% NaCl solution. They

[*] *Corresponding author*
Tel: +98 313 391 5735, Fax: +98 313 391 2752
E-mail: m.atapour@cc.iut.ac.ir
Address: Department of Materials Engineering, Isfahan University of Technology, Isfahan 84156- 83111, Iran
1. Assistant Professor
2. PhD Student
3. Professor

found that in contrast to the reduction of the uniform corrosion resistance of ultrafine grained 304 stainless steel, the grain refining improved the pitting corrosion resistance. In another attempt, Hamada et al. [15] demonstrated that the pitting corrosion resistance of the submicron grained microstructure of AISI 301LN austenitic stainless steel was improved, as compared to its coarse grained counterpart in the acidic chloride solution and also, in immersion in the ferric chloride solution. They have also reported that the general corrosion resistance of 301LN steel predominantly depends on the cold working and annealing conditions. Furthermore, Wang and Li [17] revealed that the nanocrystalline 304SS surface made by sandblasting and annealing process exhibited better passive film properties than the as-received and sandblasted specimens in the 3.5% NaCl solution. However, Zheng et al. [18] found that the thickness and composition of the passive film formed in air at room temperature on both as-received and nanocrystalline 304 stainless steels fabricated by equal channel angular press (ECAP) were very similar.

Also, Ye et al. [19] studied the corrosion performance of nanocrystallized 309 stainless steel coating prepared by DC magnetron sputtering; it was shown that the corrosion resistance of the nanocrystallized samples strongly depended on the composition of the solutions.

More recently, a number of studies were conducted to understand the correlation between the grain size and corrosion properties of austenitic stainless steels. For instance, Balusamy et al. [20] reported that surface nanocrystallization by mechanical attrition treatment (SMAT) could be beneficial in promoting the passivation of 304 SS in 0.6 M NaCl. Corrosion studies performed by Jinlong and Hongyun [14] also showed that the corrosion resistance of the ultrafine grained 321 stainless steel obtained by cold rolling and reversion annealing was lower than that of the coarse grain sample in 0.1 M NaCl solution. In contrast, superior corrosion resistance was observed in H_2SO_4 solution in the case of the ultrafine grained 321 stainless steel. They also demonstrated that the electrochemical properties of the coarse grain and the ultrafine grained 321 stainless steel were very similar in borate buffer solution.

According to these research works, it can be concluded that the existing literature is contradictory and the impact of grain size on the corrosion response of stainless steels has not yet been well understood. Furthermore, it has been demonstrated that the processing and processing rout play an important role in grain refinement and hence, the corrosion performance of materials. Thus, further work is needed to thoroughly determine the relationship between grain size and the corrosion resistance of austenitic stainless steels.

The objective of this work was to simultaneously evaluate the effect of grain size and martensitic transformation on the corrosion resistance of AISI 304L stainless steel. For this purpose, stainless steel with different grain sizes was obtained by heavily cold rolled and phase reversion annealing. In particular, the pitting corrosion behavior of 304L stainless steel with different grain sizes was investigated in 0.1M HCl solution. Meanwhile, the relationship between the grain size and the stability of the passive film was studied using electrochemical impedance spectroscopy (EIS).

2. Experimental Methods

2.1. Sample preparation

The material used in this investigation was AISI 304L stainless steel in sheet form with the thickness of 10 mm. The chemical composition of this steel is presented in Table 1. Cold rolling was carried out up to 80% at the temperature of -15 ˚C. A laboratory rolling mill with a loading capacity of 25 tons was used in this work. The cold rolled samples were subsequently annealed for reversion transformation at 900 ˚C. In order to obtain different grain sizes, five various soaking times were selected for annealing as summarized in Table 2. Following annealing, the samples were water quenched.

X-ray diffraction (XRD) measurements (Philips X'pert diffractometer with Cu Kα radiation) were performed on different samples to determine the phase constituent. A Philips XL-30 scanning electron microscope (SEM) was also used for the microstructural assessment. The microstructures of different samples were also evaluated by optical microscope (EPIPHOT 300). Etching was carried out at 1-2 V for about 10- 60s using a solution mixture of 65 ml nitric acid and 35 ml distilled water to reveal the austenite grain boundaries. The grain sizes were measured by Image J analysis software using the intercept method.

Table 1. Chemical compositions (wt. %) of the AISI 304L austenitic stainless steel employed in this study.

Element	C	Cr	Ni	Mo	Mn	Si	P	S	Co	Cu	V	Fe
wt. %	0.026	18.35	8.01	0.15	1.24	0.323	0.024	0.005	0.129	0.24	0.1	Remain

Table 2. The thermo-mechanical process conditions used in this investigation to achieve ultrafine grained structures with different grain sizes.

Sample	Cold Work (%)	Annealing temperature (°C)	Annealing time (min)	Grain Size (μm)
UFG-0.5			1	0.5 ± 0.04
GR-1			1.5	1 ± 0.2
GR-3	80	900	5	3.1 ± 0.4
GR-6			60	6.6 ± 0.7
GR-12			180	11.5 ± 1.1

UFG: Ultrafine grained, GR: Grain refined

2.2. Electrochemical tests

The electrochemical measurements were carried out with a conventional three-electrode cell system in 0.1 M HCl solution. An Ag/AgCl electrode and a platinum electrode were used as the reference and counter electrodes, respectively. All electrochemical experiments were performed using a model PARSTAT 2273 potentiostat/galvanostat. The corrosion behavior of samples with different grain sizes was assessed by open circuit potential (OCP)–time measurement, potentiodynamic polarization and electrochemical impedance spectroscopy (EIS) studies in 0.1M HCl solution at room temperature. Before all corrosion assessments, the specimens were abraded up to 1200 grit with SiC. After that, all samples were degreased in acetone, rinsed with distilled water, and dried in hot air.

The potentiodynamic polarization measurements were carried out with a scan rate of 1 mVs^{-1} in a potential range from -250 to +250 mV, relative to the EOCP. The cyclic polarization tests were accomplished according to ASTM G61 at a scan rate of 1 $mV.s^{-1}$ by starting scanning electrode potential from an initial potential of 250 mV below the open circuit potential (OCP) up to 0.5 V. The scanning direction was reversed at a limited current density of 5 $mA.cm^{-2}$.

The EIS measurements were carried out in the frequency range of 100 kHz–10 mHz and 10 mV peak-to-peak voltage amplitude versus open circuit potential (OCP). The experimental EIS data was analyzed utilizing the Z view software.

To confirm the accuracy of electrochemical measurements, all experiments were repeated at least three times and the average results were presented. All experiments were started after 1500 s immersion in electrolyte to reach the steady state open circuit potential (E_{ocp}).

In order to obtain more details regarding the corrosion performance of different samples, immersion tests were carried out in accordance with ASTM G31 standard method. The morphology of the surface of each specimen after 48 hour immersion in 0.1 M HCl was investigated by optical microscopy.

3. Results and Discussion

3.1. Microstructural characterization

Fig. 1 shows the microstructure of the as-received 304L stainless steel employed in the present study. As can be seen, the microstructure of the as-received steel consisted of equiaxed austenite grains, with an average size of 35 μm, and a small amount of δ-ferrite in the grain boundaries (shown by the dark lines in Fig. 1).

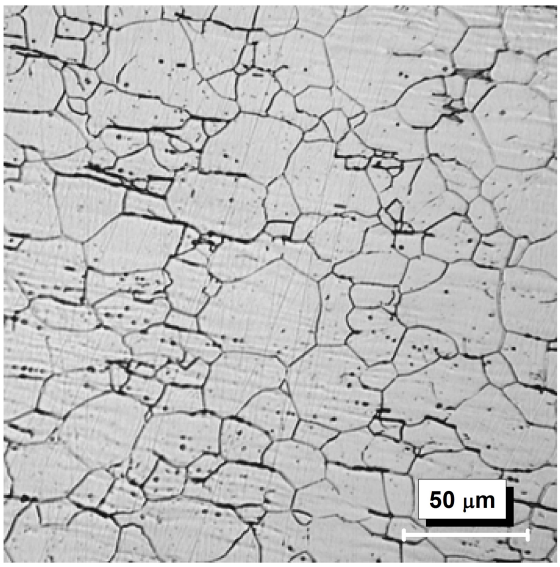

Fig.1. The microstructure of the as-received 304L stainless steel employed in the present study.

Fig. 2 displays the XRD patterns of the as-received and 80% cold rolled specimens. These X ray diffraction data revealed that the as-received steel was almost fully austenitic and after 80% rolling reduction, only ά martensite peaks consisting of ά (110), ά (200), and ά (211) were apparent.

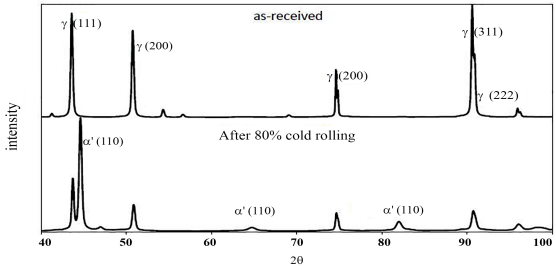

Fig. 2. The XRD patterns for as-received and 80% cold rolling samples.

In the present investigation, the annealing process was performed at 900 ˚C for the soaking times of 1, 1.5, 5, 60 and 180 minutes to obtain different grain sizes. The microstructure of the ultra-fine grain (UFG) and different grain refined samples can be seen in Figs. 3 and 4, respectively. Table 3 summarizes the variation of the grain size of the 304L stainless steel with the change of the annealing time. As shown, a considerable grain refinement was achieved via thermomechanical processing and the grain size of 304L austenitic stainless steel was decreased from 35 μm to about 500 nm equiaxed grains. Furthermore, as expected, the average grain size was increased with increasing the annealing time. Another noteworthy point was that a bimodal structure consisting of small and large grains was formed due to deformation discontinuities in the rolled samples.

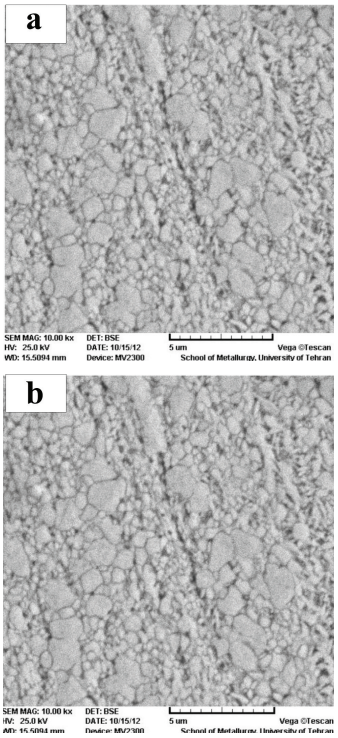

Fig. 3. Scanning electron micrographs of the ultrafine grained 304L stainless steel (500 nm grain size) in (a) high and (b) low magnifications.

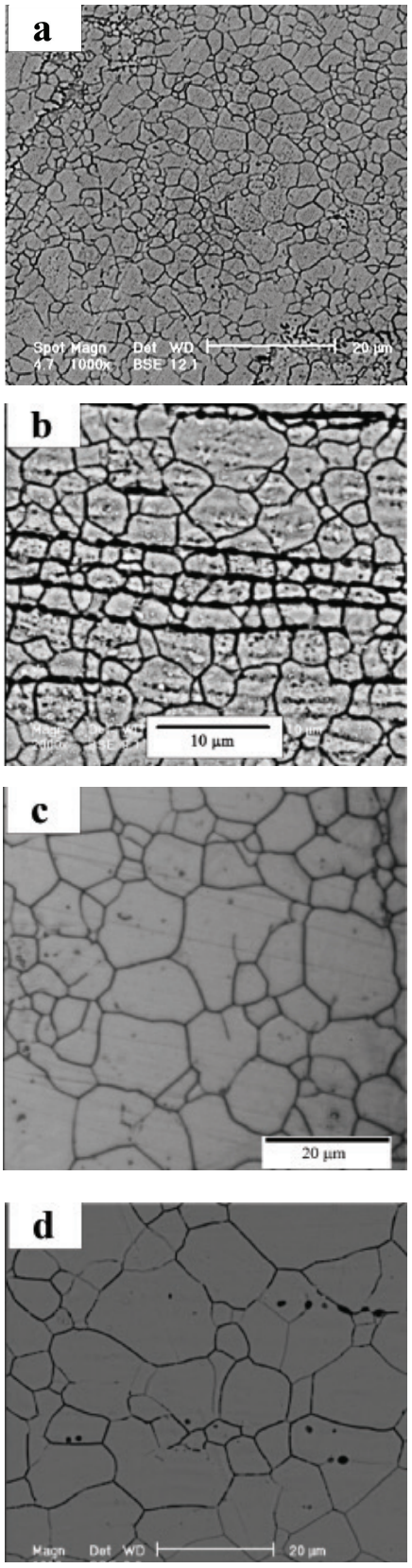

Fig. 4. The microstructures of various grain refined steels after reversion annealing at 800 °C for: (a) 1.5 min (1 μm grain size 1); (b) 5 min (3.1 μm grain size); (c) 60 min (6.6 μm grain size); (d) 180 min; and (11.5 μm grain size).

3.2. Electrochemical characterization

The variations of open circuit potential (OCP) with immersion time in 0.1 M HCl are shown for different grain sizes in Fig. 5. The OCP values of different samples were shifted towards more noble potentials, indicating that the passive film formation had occurred in 0.1 M HCl. The steady state open circuit potential was established after about 30 min, mainly due to the equal processes of the film formation and dissolution. The OCP-time plots exhibited a similar variation trend for different grain sizes. Jinlong and Hongyun [14] have recently reported similar observations for coarse-grained and ultrafine-grained (320 nm) samples of the 321 stainless steel in 0.5 M H_2SO_4 and borate buffer solutions.

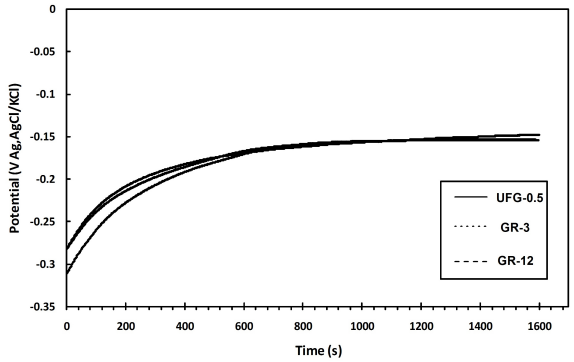

Fig. 5. Open circuit potential (OCP) plots of specimens with different grain sizes obtained in the 0.1 M HCl solution.

Potentiodynamic polarization curves for different samples in 0.1 M HCl solution are displayed in Fig. 6. It is evident that all samples exhibited similar polarization curves, thereby indicating no significant difference in the polarization behavior between the different samples. It should be emphasized that all experiments were reaped more than three times. As can be seen, the cathodic branches showed a Tafel behavior, evidencing that the cathodic hydrogen evolution reaction was activation controlled. It should be noted that hydrogen evolution is the dominant cathodic process in the corrosion of steels in acidic aqueous solutions [21]. The corrosion potential (Ecorr) of all samples was almost identical (about -0.31± 0.02 $V_{Ag/AgCl}$). As expected, the formation of Fe, Cr, and Ni oxides led to spontaneous passivation after immersion in solution [15]. The corrosion current densities (I_{corr}) obtained from the polarization curves are summarized in Table 3. The values of i_{corr} were determined by Tafel extrapolating method. Interestingly, all samples exhibited similar corrosion current density. Therefore, it could be concluded that the grain refinement obtained by martensitic process had little effect on the uniform corrosion resistance of the 304 SS in 0.1 M HCl. Similarly, work on submicron-grained 301LN austenitic stainless steel prepared by the reversion annealing of severely cold-rolled strips presented by Hamada et al. [15] indicated that E_{corr}, I_{corr} and OCP values were quite similar in 1M NaCl + 0.1M HCl solution for different grain size structures annealed at 800 ˚C. However, they reported that the presence of strain-induced martensite produced by cold rolling decreased the corrosion resistance of the 301LN in an acidic chloride medium.

Table 3. Corrosion current density of samples with different grain sizes.

Sample	Corrosion current density (μA/cm^2)
UFG-0.5	3.5 ± 0.02
GR-1	3.3 ± 0.08
GR-3	4.2 ± 0.12
GR-6	4 ± 0.08
GR-12	4 ± 0. 10

In order to establish the correlation between the grain size and the pitting susceptibility, cyclic polarization experiments were performed on the ultrafine grained 304L SS in 0.1 M HCl. Fig. 6 shows typical cyclic polarization curves obtained for the samples 1, 3 and 5 in 0.1 M HCl. Some current fluctuations took place from OCP to about 600 mV_{OCP}, evidencing metastable pitting occurrence due to the activity of chloride ions [22]. Subsequently, the current was sharply increased with increasing the potential, demonstrating the breakdown of the protective passive layer and the initiation of the pitting attack. As shown, the pitting potential (E_{pit}), which was associated with the initiation of stable pits, was significantly dependent on the microstructure morphology and grain size. The higher value of Epit represents the superior resistance of the material to pit formation. Alternatively, the repassivation potential (E_{rp}) is the potential where the forward and reverse sweeps cross, thereby indicating surface repassivation. The nobler Erp corresponds to the higher resistance of the material to pit propagation. The existence of a positive hysteresis loop indicates that the material is susceptible to the pitting corrosion. Generally, it can be concluded that the larger the positive hysteresis loop, the more difficult the repassivation.

Cyclic polarization results of samples with different grain sizes have been summarized in Table 4. The repassivation potential recorded for all samples was similar (20 mV). According to Fig. 6 and Table 4, it could be deduced that all specimens examined in the 0.1 M HCl were susceptible to pitting corrosion. It

could also be inferred that the smaller the grain size, the nobler the pitting potential. A wider hysteresis loop and consequently, inferior pitting resistance, were obtained for the 316l specimen with the grain size of 12 μm. Among all specimens, the ultra-fine grained steel with the grain size of 500 nm exhibited the best pitting corrosion resistance. These observations were in agreement with the results reported by Schino [16] for the 304 austenitic stainless steel.

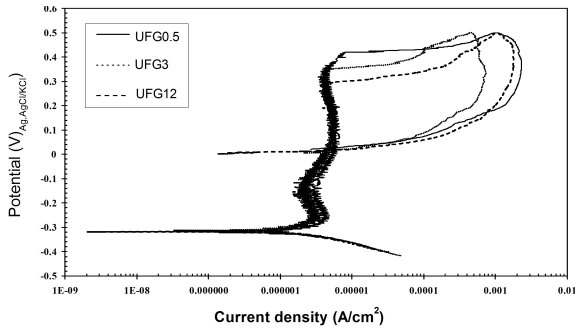

Fig. 6. Cyclic polarization curves obtained in the 0.1M HCl solution.

Table 4. Pitting potential of different samples measured from cyclic polarization curves.

Sample	Pitting Potential (mV)
UFG-0.5	420 ± 25
GR-1	390 ± 20
GR-3	370 ± 20
GR-6	320 ± 25
GR-12	290 ± 20

To confirm the results obtained by cyclic polarization measurements, the optical microstructures of the samples after 48 hours immersion in 0.1 M HCl solution are illustrated in Fig. 7. It could be seen that the size and the number of pits were decreased by increasing the grain size. Consequently, grain refinement decreased the extent of the susceptibility of the 304L stainless steel. In other words, these observations confirmed that the ultra-fine grained steel (500 nm grain size) exhibited superior pitting resistance, as compared to the steel with the larger grain size (1 μm, 3 μm, 6 μm and 12 μm).

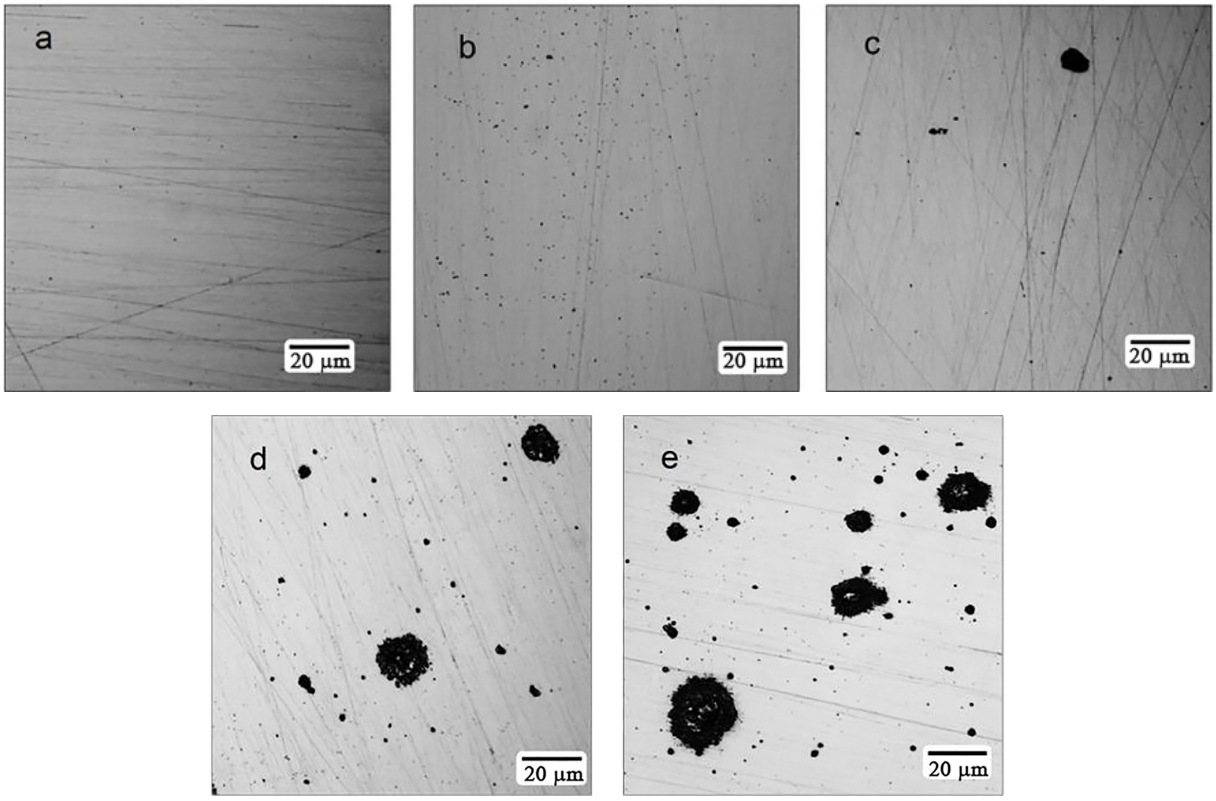

Fig. 7. Optical micrographs of the corroded samples after 48 hours immersion in the 0.1M HCl solution: (a) UFG-0.5, (b) GR-1, (c) GR-3, (d) GR-6, and (e) GR-12.

The correlation between the grain refinement and the failure resistance of the passive film formed on the surface of stainless steels was investigated according to the surface electron work function (EWF) [17, 23]. It has been demonstrated that the electrochemical stability of a surface, which represents its resistance to corrosion attack, is improved with decreasing the grain size of the 304 stainless steel using a sandblasting and annealing process [17]. Therefore, the passive film formed on the specimen with the grain size of

500 nm exhibited the highest failure resistance among all specimens.

As it is well established, the grain size refinement leads to increasing diffusion paths, thereby facilitating the transportation of Cr onto the surface of the specimen and forming a more homogeneous passive film rich in Cr [13, 19]. However, some authors have claimed increased rates of general corrosion as grain sizes are decreased due to passive film destabilization [13]. For example, Balusamy et al. [20] have reported that the surface nanocrystallization induced by surface mechanical attrition treatment (SMAT) can deteriorate the corrosion resistance of AISI 409 grade stainless steel in 0.6 M NaCl. This behavior could be attributed to the formation of defective interfaces and defects in grains resulting from the accumulation of internal stresses [20]. A similar trend has been demonstrated for AISI 316L stainless steel in 0.05 M H_2SO_4 + 0.25 M Na_2SO_4 [24]. It is worthwhile to note that the density of dislocations could also influence the passivation process by providing more diffusion paths for elements to migrate to the surface [25]. However, as demonstrated in the present work, the pitting corrosion resistance of the ultrafine grained 304L stainless steel produced by martensitic process was improved significantly in 0.1 M HCl. It seems, therefore, that the oversaturation of martensite by carbon and the fast diffusion of chromium in this phase can improve rehomogenization phenomenon and facilitate the rapid formation of a uniform passive film [26]. So, it appeared that the martensitic transformation could also be a reason for improving the corrosion performance of the ultrafine grained 304L in this investigation. Furthermore, it has been demonstrated that the grain refinement can decrease the adsorption ability of Cl^- on the surface of the material and then enhance the pitting corrosion resistance [27].

In order to evaluate the stability of the passive film formed on different ultrafine grained 304L stainless steels, electrochemical impedance spectroscopy (EIS) was carried out. These measurements were performed at OCP after samples were immersed in 0.1 M HCl solution for 1500 seconds (Fig. 8). Typical Nyquist plots, as illustrated in Fig. 8a, revealed the partial semi-circle Nyquist curves for all specimens. The Nyquist plots were depressed semicircles. It is worthwhile to note that the appearance of depressed semicircles could be related to such inhomogeneities as impurity, and grain and sub-grain morphology of the surface for depressing semicircles [28]. Furthermore, the similar Bode plots (Fig. 8b) implied that different samples underwent the same corrosion behavior.

It could be observed that the partial circle was decreased with the increase of grain size, thereby indicating the reduced impedance of the passive film.

Several models of circuits were employed to fit the experimental data. The best equivalent circuit model compatible with the Nyquist plots is depicted in Fig. 9.

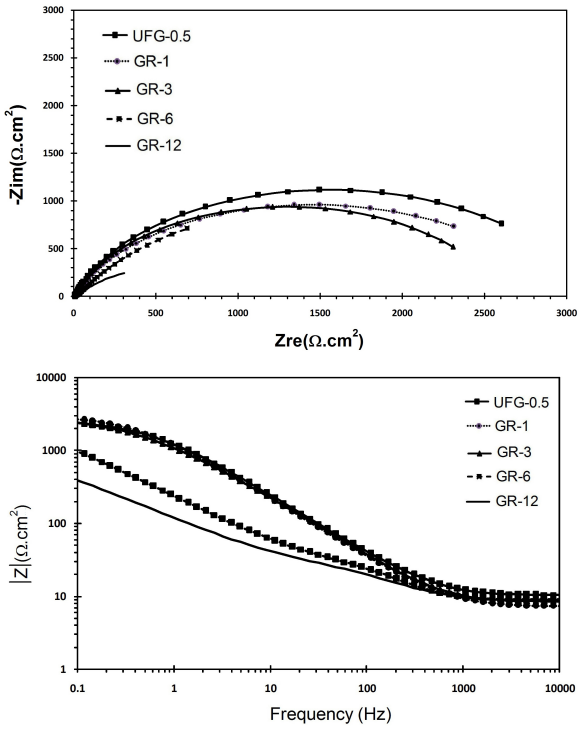

Fig. 8. Experimental EIS data of specimens with different grain sizes, (a) Nyquist, and (b) Bode plots after 1600s immersion in the 0.1M HCl solution.

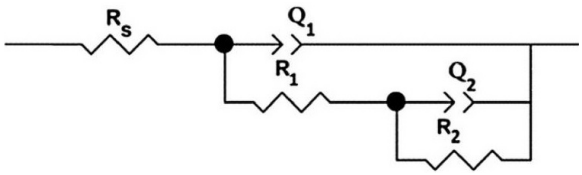

Fig. 9. Equivalent circuit used for the analysis of impedance spectra in this investigation.

A similar equivalent circuit has been proposed by other authors for different stainless steels in acidic solutions [29, 30]. This equivalent circuit consists of two time constants. The first time constant revealed at the higher frequencies is related to the formation of a defective passive film, where R1 is the passive film resistance and Q1 is the constant phase element of the passive film [31]. The second time constant (R_2Q_2) corresponding to the lower frequencies is attributed to the transport phenomenon of reactants through the porosities of the passive film [31, 32]. The symbol Q is employed to explain the non-ideal capacitance behaviors due to different physical phenomena such as surface heterogeneity [31]. The impedance of the constant phase element (CPE) is represented by [33].

$$Q=ZCPE\ (\omega)=Z0(i\omega)^{-n} \qquad \text{Eq. (1)}$$

, where Z_0 is a constant, ω is the angular frequency

(rad s^{-1}), and n ($0 \leq n \leq 1$) is defined as a CPE power. Depending on the value of the exponent n, CPE may represent a resistance, R(n = 0), a capacitance, C(n = 1), a Warburg impedance, W(n = 0.5), or an inductance, L(n = -1) [33]. Fig. 10 illustrates a typical plot of experimental data and simulated data, thereby showing that the fitting is good for all frequency domains. The fitted parameters are presented in Table 5. It can be concluded that R_1 and R_2 and subsequently, the polarization resistance ($R_p=R_1+R_2$) are increased with decreasing the grain size. This confirms that the grain refinement can have a great influence on the stability of the passive film.

However, it is obvious that the most important impact of grain refinement on the corrosion performance is improving the passive film resistance (R_1). Furthermore, the higher R_1 obtained for the specimen with the lowest grain size (3225 Ω cm^{-2}) indicated that its passive film was less defective [34]. Meanwhile, it is well demonstrated that the capacitance is inversely proportional to the thickness of the double layer [35]. Therefore, according to Table 5, it could be deduced that the thickness of the passive film formed on the 304L specimens was increased by decreasing the grain size. It might be due to the fast diffusion of elements forming a compact film on the surface of the specimen with a lower grain size [27].

The values of the exponent n, as obtained by fitting the EIS data, were lower than unity for all studied samples, indicating the presence of heterogeneities at the interfaces and static disorders such as porosity in the passive film of different samples. However, grain refinement increased the value of the exponent n_1, indicating the reduction of passive film surface inhomogeneity.

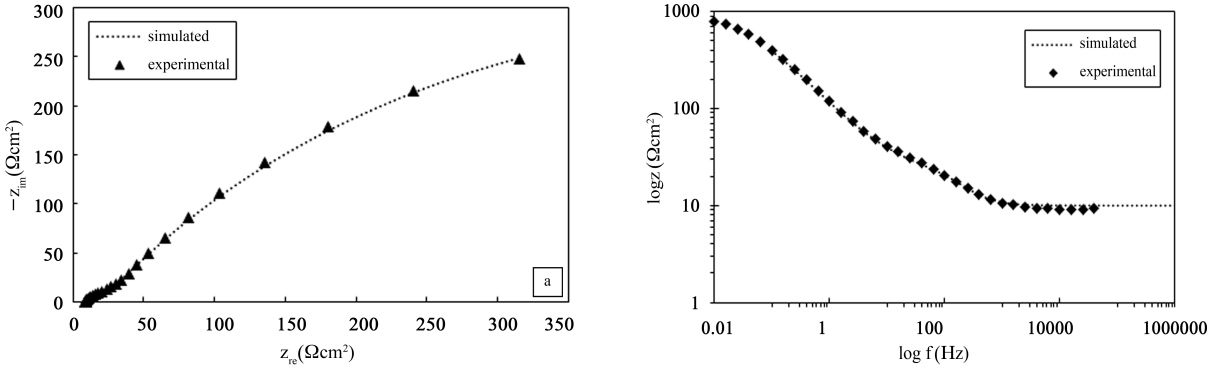

Fig. 10. Experimental and fitted EIS data of GR-12, (a) Nyquist, and (b) Bode plot after 1 h immersion in the 0.1M HCl.

Table 5. Fitting results of EIS plots in the 0.1M HCl.

Sample	R_S (Ω.cm²)	Q1 (μF.cm^{-2})	n_1	R1 (Ω.cm²)	Q2 (μF.cm^{-2})	n_2	R2 (Ω.cm²)
UFG-0.5	3	31	0.99	3225	120	0.72	31
GR-1	2.5	37.5	0.97	3140	145	0.71	33
GR-3	3	45.3	0.98	2943	173	0.65	29.7
GR-6	3.5	60.5	0.97	2582	1120	0.68	25.6
GR-12	3	107	0.94	1108	2550	0.65	17.7

4. Conclusions

In this investigation, the effects of grain size and martensitic transformation on the corrosion behavior of 304L stainless steel were studied. From the experiments, the following conclusions could be drawn:

- Potentiodynamic evaluations conducted in 0.1M HCl solution demonstrated that grain size variation had little effect on the corrosion potential and corrosion current density of the 304L stainless steel.
- The results of cyclic polarization tests revealed that a wider hysteresis loop and consequently, an inferior pitting resistance were obtained for the 316l specimen with the larger grain size.
- Optical micrographs recorded on the surface of different samples after 48 hours immersion in 0.1M HCl revealed that the size and the number of pits were decreased by increasing the grain size.
- Based on the EIS observations, the passive film

formed on the specimen with the grain size of 500 nm exhibited the highest failure resistance among all speciment.

References

[1] J. Beddoes and J. G. Parr: Introduction to stainless steels, 3rd. Technology & Engineering, ASM International, (1999).
[2] D. A. Jones: Principles and prevention of corrosion, 2nd ed., Prentice Hall, London. (1996).
[3] C.-O. Olsson and D. Landolt: Electrochim. Acta, 48 (2003), 1093.
[4] S. Rudenja: Sur. Coat. Technol. 114 (1999), 129.
[5] H.-P. Feng , C.-H. Hsu, J.-K. Lu and Y.-H. Shy: Mater. Sci. Eng., A 347 (2003), 123.
[6] R. A. Antunes, A. C. D. Rodas, N. B. Lima, O. Z. Higa and I. Costa: Sur. Coat. Technol., 205 (2010) , 2074.
[7] Q. Pan, W. Huang, R. Song, Y. Zhou and G. Zhang: Sur. Coat. Technol., 102 (1998) , 245.
[8] M. Lei and Z. Zhang: J. Vac. Sci. Technol. A 15 (1997) , 421.
[9] L. Gil et al.: Sur. Coat. Technol., 201 (2006) , 4424.
[10] F. Humphreys and M. Hatherly: Recrystallization and related annealing phenomena, Elsevier (1995).
[11] F. Forouzan, A. Najafizadeh, A. Kermanpur, A. Hedayati and R. Surkialiabad: Mat. Sci. Eng., A 527 (2010) , 7334.
[12] K. Tomimura, S. Takaki and Y. Tokunaga: ISIJ Int., 31 (1991) 1431.
[13] K. Ralston and N. Birbilis: Corrosion 66 (2010) , 075005.
[14] L. Jinlong and L. Hongyun: Appl. Sur. Sci., 280 (2013) , 124.
[15] A. S. Hamada, L. P. Karjalainen and M. C. Somani: Mater. Sci.Eng., A 431 (2006) , 211.
[16] A. Di Schino and J. Kenny: J. mater. sci. let., 21 (2002) , 1631.
[17] X. Wang and D. Li, Wear, 255 (2003), 836.
[18] Z. J. Zheng, Y. Gao, Y. Gui and M. Zhu: Corros. Sci., 54 (2012) , 60.
[19] W. Ye, Y. Li and F. Wang: Electrochim. Acta, 51 (2006) , 4426.
[20] T. Balusamy, T. Sankara Narayanan, K. Ravichandran, I. S. Park and M. H. Lee: Corros. Sci. 74 (2013) , 332.
[21] A. S. Fouda, F. E. Heakal and M. S. Radwan: J. Appl. Electrochem., 39 (2009), 391.
[22] Y. Yang, B. Yan, J. Li and J. Wang, Corros. Sci., 53 (2011) , 3756.
[23] X. Y. Wang and D. Y. Li: Mater. Sci. Eng., A 315 (2001) , 158.
[24] A. Q. Lü et al: Acta Metall. Sin. (Engl. Lett.), 19 (2006) , 183.
[25] W. D. Nix: Mater. Sci. Eng., A 234–236 (1997) , 37.
[26] H. Sidhom, T. Amadou and C. Braham: Metall. Mater. Trans., A 41 (2010) , 3136.
[27] L. Liu, Y. Li and F. Wang: J. Mater. Sci. Technol, 26 (2010) , 1.
[28] K. Jüttner: Electrochim. Acta 35 (1990) , 1501.
[29] Y. X. Qiao, Y. G. Zheng, W. Ke and P. C. Okafor: Corros. Sci., 51 (2009) , 979.
[30] A. Kocijan, D. K. Merl and M. Jenko: Corros. Sci., 53 (2011) , 776.
[31] R. G. Kelly, J. R. Scully, D. Shoesmith and R. G. Buchheit, Electrochemical techniques in corrosion science and engineering, CRC Press (2002).
[32] C. Liu, Q. Bi, A. Leyland and A. Matthews: Corros. Sci., 45 (2003) , 1243.
[33] I. D. Raistrick, D. R. Franceschetti and J. R. Macdonald: Impedance Spectroscopy. John Wiley & Sons, Inc., (2005), 27.
[34] H. Luo, C. F. Dong, X. G. Li, K. Xiao: Electrochim. Acta, 64 (2012) , 211.
[35] P. Li, J. Y. Lin, K. L. Tan and J. Y. Lee: Electrochim. Acta, 42 (1997) , 605.